AGU PUBLICATIONS

Paleoceanography

RESEARCH ARTICLE

10.1002/2015PA002847

Key Points:

- Barbados *A. palmata* SL record shows no evidence that a MWP triggered the Younger Dryas
- *A. palmata* record rate of SL rise decreased smoothly to a "slow stand" by Younger Dryas' end
- MWP-1B confirmed as a 14 {+ or -} 2 m jump in SL coincident with North Hemisphere insolation maximum

Supporting Information:

- Text S1, Figures S1 and S2, and Tables S1 and S2

Correspondence to:
N. A. Abdul,
naabdul@scarletmail.rutgers.edu

Citation:
Abdul, N. A., R. A. Mortlock, J. D. Wright, and R. G. Fairbanks (2016), Younger Dryas sea level and meltwater pulse 1B recorded in Barbados reef crest coral *Acropora palmata*, *Paleoceanography*, *31*, 330–344, doi:10.1002/2015PA002847.

Received 12 JUN 2015
Accepted 22 JAN 2016
Accepted article online 27 JAN 2016
Published online 20 FEB 2016

Younger Dryas sea level and meltwater pulse 1B recorded in Barbados reef crest coral *Acropora palmata*

N. A. Abdul[1], R. A. Mortlock[1], J. D. Wright[1], and R. G. Fairbanks[1,2]

[1]Earth and Planetary Sciences, Rutgers State University of New Jersey, Piscataway, New Jersey, USA, [2]Columbia University, New York, New York, USA

Abstract The Younger Dryas climate event occurred during the middle of the last deglacial cycle and is marked by an abrupt shift in the North Atlantic polar front almost to its former glacial position, trending east to west. Using high-precision and high-accuracy U-Th-dated Barbados reef crest coral, *Acropora palmata*, we generate a detailed sea level record from 13.9 to 9000 years before present (kyr B.P.) and reconstruct the ice volume response to the Younger Dryas cooling. From the mid-Allerød (13.9 kyr B.P.) to the end of the Younger Dryas (11.65 kyr B.P.), rates of sea level rise decreased smoothly from 20 mm yr^{-1} to 4 mm yr^{-1}, culminating in a 400 year "slow stand" before accelerating into meltwater pulse 1B (MWP-1B). The MWP-1B event at Barbados is better constrained as beginning by 11.45 kyr B.P. and ending at 11.1 kyr B.P. during which time sea level rose 14 ± 2 m and rates of sea level rise reached 40 mm yr^{-1}. We propose that MWP-1B is the direct albeit lagged response of the Northern Hemisphere ice sheets to the rapid warming marking the end of the Younger Dryas coinciding with rapid warming in the circum-North Atlantic region and the polar front shift from its zonal to meridional position 11.65 kyr B.P. As predicted by glaciological models, the ice sheet response to rapid North Atlantic warming was lagged by 400 years due to the thermal inertia of large ice sheets. The regional circum-North Atlantic Younger Dryas climate event is elevated to a global response through sea level changes, starting with the global slowdown in sea level rise during the Younger Dryas and culminating with MWP-1B. No meltwater pulses are evident at the initiation of the Younger Dryas climate event as is often speculated.

1. Introduction

Milankovitch [1941] correctly deduced that changes in incoming solar radiation to the higher northern latitudes, controlled by subtle variations in the Earth's orbit, paced the growth and decay of continental ice sheets. Direct support for orbital forcing of climate comes from deep-sea cores [*Hays et al.*, 1976] and dated uplifted coral reef terraces on Barbados [*Broecker et al.*, 1968; *Mesolella et al.*, 1969]. For more than a century, botanists, glaciologists, and geologists have documented a curious pause midway through the last deglaciation that was marked by an abrupt return to glacial-like conditions in the circum-North Atlantic region. Known as the Younger Dryas Chronozone, this cold period was originally assigned to the time interval between 11,000 and 10,000 radiocarbon years before present (B.P.) [*Mangerud et al.*, 1974] which, when calibrated, corresponds in time to 13,000–11,700 calendar years before present (kyr B.P.) [*Fairbanks*, 1990]. More precise and accurate dating and annual layer counting in the North Greenland Ice Core Project (NGRIP) ice cores constrain a local atmospheric temperature or air mass shift, as expressed in the $\delta^{18}O$ of ice, from 12.85 to 11.65 kyr B.P. [*Rasmussen et al.*, 2006], corresponding to the Younger Dryas stadial. Although widely accepted as the type example of Younger Dryas Chronozone, it remains a local Greenland chronology.

The Younger Dryas is one of the most studied intervals of Earth's climate history for several reasons. First, it is perhaps the best example of large-scale climate instability on millennial time scales. Second, it can be radiometrically dated to high precision and high accuracy by several dating methods. Third, abundant proxy records contain evidence of this event throughout the circum-North Atlantic in the ocean, on land and lakes, and in the Greenland ice sheet. Fourth, understanding the causes of this climate event may lead to a better understanding of the amplifiers of climate change or at least identify the regions and systems most sensitive to climate instabilities in the past and possibly in the future.

There is evidence that during the Younger Dryas North Atlantic polar surface waters and sea ice boundaries extended further south spreading eastward in less than a century [*Ruddiman and McIntyre*, 1981], reflecting a

shift from more meridional (southwest to northeast) to more latitudinal (east to west) atmospheric and surface ocean circulation in the North Atlantic. These circulation changes coincided with regional cooling in the circum-North Atlantic southward to lower temperate latitudes (34°N to 45°N), identified in deep-sea sediment core records by sharp increases in % *N. pachyderma* (sinistral) and ice-rafted debris [*Ruddiman and McIntyre*, 1981; *Keigwin and Lehman*, 1994], North American and European pollen records [*Watts*, 1980; *Peteet*, 1995], European lake sediments [*Björck et al*., 1996; *Brauer et al*., 1999], and climate change marker species [*Lemdahl*, 1991; *Ponel et al*., 2007]. Younger Dryas-age glacial landforms chronicle a cessation of ice sheet retreat and in some regions a readvance of alpine glaciers and ice fronts across already deglaciated areas of the maritime Fennoscandian region (Norway, Sweden, and Finland) [*Andersen et al*., 1995; *Rainio et al*., 1995; *Kleman et al*., 1997; *Boulton et al*., 2001]. Synchronous with Fennoscandian ice sheet resurgence were less pronounced glacier readvances in areas of the Laurentide ice sheet proximal to the North American Great Lakes [*Lowell et al*., 1999] in regions of the eastern Canadian Arctic such as Baffin Island and Lake Champlain [*Miller*, 1980; *Lasalle and Shilts*, 1993], Scotland [*Sutherland et al*., 1993] and along some margins of the Greenland ice sheet [*Simpson et al*., 2009].

In advancing a triggering mechanism for the Younger Dryas, paleoceanographers have argued for changes in sea ice distribution [*Ruddiman and McIntyre*, 1981] and/or reduction in North Atlantic Deep Water (NADW) export thereby reducing the northward flow of warm tropical waters via the Gulf Stream [*Weyl*, 1968; *Rooth*, 1982; *Broecker and Denton*, 1989], while atmospheric scientists have argued that changing ice sheet geometries created temporary splits or shifts in the North American Jet Stream [e.g., *Manabe and Broccoli*, 1985], amplified by highly zoned winds promoting a deeply mixed surface ocean, as more plausible explanations [*Seager et al*., 2002; *Wunsch*, 2002].

The transition into the Younger Dryas is often described as "abrupt," and multiple atmospheric climate proxies within the Greenland ice core layers indicate that the onset occurred over decades in several steps [*Alley*, 2000; *Rasmussen et al*., 2006] consistent with the "flickering" associated with atmospherically driven perturbations [*Taylor et al*., 1993]. The δ^{18}O records of Greenland ice cores indicate that the decrease began around 12.85 kyr B.P. and reached a temperature minimum around 12.7 kyr B.P. [*Rasmussen et al*., 2006] when Greenland surface temperatures had cooled by 5 to 10°C [*Cuffey and Clow*, 1997; *Severinghaus et al*., 1998]. δ^{18}O shifts in Greenland ice cores are commonly interpreted solely as a temperature indicator [*Jouzel et al*., 1987; *Dansgaard et al*., 1993]; however, *Charles et al.* [1994] note that δ^{18}O shifts also reflect changes in air mass sources and their water vapor mixing histories. A varved lake sediment record from western Germany supports the multidecadal climate decline into the Younger Dryas, with the final shift into full stadial mode identified at that location at 12.68 kyr B.P. [*Brauer et al*., 2008]. The termination of the Younger Dryas in Greenland is more abrupt than the inception and is identified by an ~5 to 10°C increase in surface temperatures [*Taylor et al*., 1997; *Severinghaus et al*., 1998; *Alley*, 2000] or an air mass shift [*Charles et al*., 1994] and abrupt disappearance of sea ice south of Newfoundland (~47°N latitude) by 11.6 kyr B.P. [*Pearce et al*., 2014].

Ironically, the Younger Dryas cold interval occurred during Northern Hemisphere radiation maximum and in the middle of the most recent deglaciation. These large swings in circum-North Atlantic climate associated with the initiation and termination of the Younger Dryas stand in sharp contrast to slowly changing deglacial forcing, such as increasing Northern Hemisphere summer insolation [*Berger and Loutre*, 1991], vigorous North Atlantic overturning [*McManus et al*., 2004], and possibly the impact of rising atmospheric CO_2 [*Monnin et al*., 2001], CH_4 [*Brook et al*., 2000; *Marcott et al*., 2014], and sea level [*Fairbanks*, 1989]. Although considerable debate surrounds speculation that the Younger Dryas was a global event (see extensive reviews by *Peteet* [1995] and *Björck* [2007]), the conundrum created by the apparent decoupling of circum-North Atlantic proxy records documenting the Younger Dryas cooling versus evidence for a warming and deglaciating planet has led some to advocate for regional catastrophic triggers. A sudden release of meltwater from the Laurentide ice sheet, triggered by either a natural breach of proglacial Lake Agassiz's ice dam [*Broecker et al*., 1989] or a destabilization and demise of the Laurentide ice sheet triggered by an extraterrestrial impact [*Firestone et al*., 2007], are two such catastrophic mechanisms proposed to have initiated Younger Dryas cooling.

The "flood or meltwater hypothesis" posits that the Younger Dryas stadial was caused by a sudden discharge of a large volume of glacial meltwater that freshened and stratified the North Atlantic, disrupted NADW formation, and reduced or shutdown the Atlantic Meridional Overturning Circulation (AMOC) [*Broecker et al*., 1985, 1989]. Supporting evidence for the "flood hypothesis" from surface ocean studies is lacking; however,

several deep water proxy records from North Atlantic cores indicate possible disruption of NADW production [*McManus et al*., 2004; *Piotrowski et al*., 2005; *Elmore and Wright*, 2011]. The retreat of the North American ice sheet past the continental divide [*Teller*, 1995], coupled with isostatic adjustments associated with deglaciation, are proposed to have led to the rerouting of meltwater from the Gulf of Mexico via the Mississippi River eastward into the mid-Atlantic via the St. Lawrence River [*Broecker et al*., 1989].

Meltwater additions to the surface ocean are most commonly identified, traced, and reconstructed using δ^{18}O records generated from planktonic foraminifera in marine deep-sea cores and dated using the radiocarbon chronometer [e.g., *Fairbanks et al*., 1992; *Keigwin and Lehman*, 1994; *Flower et al*., 2004]. Planktonic foraminiferal oxygen isotope records obtained from deep-sea cores taken in the mid-Atlantic region [*Keigwin and Lehman*, 1994] and in the Gulf of Mexico [*Flower and Kennett*, 1990] were cited in support of changing outflow pathways, with meltwater discharge-driven minima in δ^{18}O values correlated to the mid-Atlantic and Gulf of Mexico approximately synchronous Heinrich 1 Event [*Bond et al*., 1992] and the initiation of the Younger Dryas, respectively. Stratigraphic and structural field evidence for this levee breach, however, is lacking [*Lowell et al*., 2005], and revised paleotopographic reconstructions of the Lake Agassiz region no longer support a mid-Atlantic meltwater discharge coincident with the onset Younger Dryas [*Teller et al*., 2005].

Condron and Winsor [2012] revisited the feasibility of meltwater released into the mid-Atlantic via the St. Lawrence River catastrophically impacting NADW formation in the circum-North Atlantic. In their experiments, 5 sverdrup (Sv) (10^6 m^3/s) (~160,000 km^3 yr^{-1}) of meltwater released into the St. Lawrence River over the course of a year was quickly deflected southward by North American coastal currents, entrained into the Gulf Stream, and mixed into the Atlantic subtropical gyre as predicted by *Khatiwala et al.* [1999]. Applying freshwater forcing of similar magnitude but instead, rerouting discharge into the Arctic Ocean via the Mackenzie River as proposed by *Tarasov and Peltier* [2005], resulted in a 30% reduction in the AMOC [*Condron and Winsor*, 2012]. However, a freshwater flux 25 times the modern annual average discharged from the Arctic Ocean catchment area (3300 km^3 yr^{-1} or ~1/10 of a sverdrup) [*Aagaard and Carmack*, 1989] was required to achieve this reduction, further weakening support for this mechanism. Still, the discovery of erosional features on the Mackenzie River delta (~13 kyr B.P.) is consistent with a pre-Younger Dryas flood [*Murton et al*., 2010] and keeps the possibility of the "Arctic Gateway" alive. Admittedly, much of the support for an ocean-based driver of the Younger Dryas climate event, as surmised by *de Vernal et al.* [1996], continues to hinge on a circum-North Atlantic that is much more sensitive to site specific meltwater input than is predicted by conceptual models. Importantly, deep water formation can occur rapidly in small regions anywhere over the wide North Atlantic and northern seas [*Yashayaev and Clarke*, 2008] and not just in modern source regions of the North Greenland and Labrador Seas.

Fairbanks [1989] showed that there were two discrete MWPs (MWP-1A and MWP-1B) bracketing the Younger Dryas that have been misinterpreted as meltwater rerouting events. Evidence for surface water freshening at the start of the Younger Dryas cannot be explained by either MWP-1A or MWP-1B, which precede and postdate the Younger Dryas climate event, respectively, by hundreds of years. Moreover, no AMOC reduction is observed during either of these two massive and well-documented circum-North Atlantic meltwater pulses [*McManus et al*., 2004; *Piotrowski et al*., 2005], suggesting that NADW formation remained robust in the face of even the largest documented meltwater pulses.

The phasing of meltwater pulses, potential disruptions to NADW formation, and changes in Greenland surface air temperature or air mass mixing ratios linked to Younger Dryas cooling require precise and accurate dating of multiple proxy records. *Fairbanks* [1989] demonstrated that the global sea level record contained in Barbados corals offered a direct measure of meltwater added to the ocean and, when dated using the U-series chronometer [*Bard et al*., 1990; *Fairbanks*, 1990; *Peltier and Fairbanks*, 2006], provided the precision and accuracy needed to detect relationships between freshwater discharge and the onset of the Younger Dryas. A record of sea level at Barbados based on U-Th-dated reef crest coral *Acropora palmata* (*A. palmata*) suggests sustained deglacial sea level rise through the Younger Dryas [*Fairbanks*, 1989, 1990; *Bard et al*., 1990], but sample resolution precluded resolving structure in the record within and bracketing the Younger Dryas. In this study, we have increased the number of Barbados *A. palmata* samples spanning the mid-Allerød to the early Holocene nearly fivefold to generate a relative sea level record with an average resolution of 60 years. Equipped with this high-resolution, deglacial sea level record, we first revisit the evidence for a freshwater trigger as an initiator of the Younger Dryas, then document the sea level response to ice sheet regeneration and demise associated with Younger Dryas cooling, and reconstruct the timing and magnitude of the second deglacial meltwater event

MWP-1B that follows the Younger Dryas climate event. Finally, we investigate the phasing between atmospheric frontal shifts, abrupt millennial-scale atmospheric oscillations (inferred from Greenland ice core records) and changes in global ice volume.

2. Study Area

2.1. Barbados Historical Perspective and Assessing Glacial Isostatic Adjustments

Located in the southern West Indies (13.17°N, 59.55°W), Barbados sits on the accretionary prism formed by the subduction of the Atlantic plate beneath the Caribbean plate. As a result, Barbados is being uplifted at a mean rate of 0.34 mm yr^{-1} [*Broecker et al*., 1968; *Matthews*, 1973; *Bender et al*., 1979; *Fairbanks*, 1989]. Since Barbados is located distal to any growing or decaying ice sheets it is generally accepted to be only negligibly impacted by glacioisostatic adjustment or ocean basin sloshing largely driven by dynamic Northern Hemisphere ice sheets [*Peltier and Fairbanks*, 2006]. The uplifted coral reef terraces on Barbados have provided ideal opportunities to study Pleistocene sea level variability [e.g., *Matthews*, 1972, 1973; *Gallup et al*., 1994, 2002; *Cutler et al*., 2003; *Thompson et al*., 2003]. *Fairbanks* [1989] further demonstrated that informed drilling of bathymetric highs on the submerged fossil coral reef terraces made it possible to resolve a detailed record of glacial to interglacial sea level change. *Fairbanks* [1989] constrained sea level at 20 kyr B.P. to 120 m below present, shallower, but consistent with the consensus CLIMAP minimum estimate of −127 m below sea level (bsl) [*CLIMAP Project Members*, 1981]. A criticism of the "dipstick method" for determining past global sea level lies in the assumption that local glacial meltwater discharge would result in an evenly distributed rise in global sea level since it is known that slow postglacial viscoelastic mantle adjustments [*Peltier*, 1974] and the instantaneous gravitational attraction (retraction) of the ocean to growing (shrinking) ice sheets [*Walcott*, 1972; *Clark et al*., 1978] can influence relative sea level at nearby and to a lesser extent, far field sites.

An analysis of relative sea level records from other far field sites such as Australia [*Yokoyama et al*., 2001] has suggested an older [*Clark et al*., 2009] or deeper [e.g., *Nakada and Lambeck*, 1988; *Yokoyama et al*., 2000] last glacial eustatic lowstand. The deviation of both the timing and the magnitude of change in eustatic sea level from the conventional −120 m at 20 kyr B.P. originally proposed by [*Fairbanks*, 1989] has led some to argue that Barbados is not immune to glacial isostatic distortions [e.g., *Yokoyama et al*., 2000; *Clark et al*., 2002]. A sea level correction of 10 m to relative sea level at Barbados for the Last Glacial Maximum (LGM) is now predicted based on glacial isostatic adjustment (GIA) modeling which incorporates the influence of a mantle viscosity on a downward thrusting slab simulating local deformation *Austermann et al.* [2013].

Understandably, a 10 m model correction to relative sea level at Barbados as proposed by *Austermann et al.* [2013] is time, ice volume, and model parameterization dependent and expected to be much smaller when applied to sea level estimates made midway through the deglaciation over a span of 4000 years. According to *Steffen et al.* [2013], GIA model sensitivity to ice-loading parameterization is significantly reduced after 13 kyr B.P., and for the time interval presented in this study (13.9 to 9 kyr B.P.), coupled ice and Earth model predictions suggest that relative sea level at Barbados exhibited little departure from eustasy [*Peltier and Fairbanks*, 2006; *Milne and Mitrovica*, 2008] and all but converges on the predicted ice-equivalent sea level estimate as illustrated in *Carlson and Clark* [2012] by 13 kyr B.P. Furthermore, isostatic adjustments associated with deglaciation occur on much longer time scales (5 to 7 kyr postglacial decay times [*Mitrovica et al*., 2000]) and cannot generate the magnitude or rapidity in the centennial-scale accelerations in the Barbados sea level record, presented and examined here.

For the reasons outlined above, no isostatic corrections were applied to the Barbados sea level data. However, care should be taken when comparing this relative sea level record with sea level records generated elsewhere as isostatic and gravitational effects will differ depending on location and modeling parameterization, including assumptions as to the source of meltwater to the ocean. We note most GIA models predict relative sea level at Barbados to lie slightly below the eustatic estimate for the time interval discussed [*Bassett et al*., 2005; *Milne and Mitrovica*, 2008].

2.1.1. Barbados Coral Reef Ecology

The low-diversity coral reefs at Barbados exhibit clearly defined depth-dependent coral zonations with the prevailing species in each zone being morphologically adapted to dominating that specific ecological niche [*Mesolella*, 1967]. The breaker zone (reef crest) is almost exclusively dominated by the constructional reef building coral *Acropora palmata*. Moving seaward from the shallow water reef crest *A. palmata* facies

(<5 m water depth), the fore reef slope zone is dominated by *Acropora cervicornis* (5 to 15 m water depth), followed by the coral head zone (>15 m) so named for the increasing abundance of stony massive corals such as *Montastrea annularis* and Faviidae spp [*Mesolella*, 1967]. The fidelity of this depth-moderated species succession is confirmed in modern reefs [*Goreau and Wells*, 1967] and in numerous roadcut exposures of the uplifted fossil reef terraces [*Mesolella*, 1967], and is similarly validated in the Barbados offshore drill cores (Figure S1 in the supporting information).

The *A. palmata* reef crest facies is ecologically restricted to the wave-impacted upper 5 m of the water column [*Goreau*, 1959; *Mesolella*, 1967] and has proven to be an excellent archive of sea level variability [*Fairbanks*, 1989; *Peltier and Fairbanks*, 2006]. Reef crest *A. palmata* are reliably distinguished by their infilled corallites. It is this morphological adaptation to living in the surf zone that bolsters the reef crest against wave action and fortuitously, for geochemical studies, reduces postmortem diagenesis of the fossil coral [*Gladfelter*, 1982]. Although individual *A. palmata* specimens exhibits growth rates ranging from 47 to 99 mm yr^{-1} [*Gladfelter et al.*, 1978], the coral reef as an ecosystem is maintained by the balance of biological, physical, and chemical erosion verses carbonate production known as reef accretion. Constructional reefs, such as those at Barbados, have modeled accretion rates ranging from 14 to 16 mm yr^{-1} [*Hubbard*, 2009]. High accretion rates, backfilled corallites, and an ecologically restricted depth habitat make the reef crest *A. palmata* arguably the best Pleistocene indicator of sea level, when sampled from the reef crest facies [*Lighty et al.*, 1982; *Fairbanks*, 1989].

Surveys conducted on Jamaican coral reefs confirmed the optimum depth range of 1 to 5 m for the reef crest *A. palmata* [*Goreau and Wells*, 1967], and while isolated *A. palmata* individuals were reported at depths up to 17 m, they should not be confused with the reef crest framework building morphotype. Importantly, occurrences of deeper dwelling *A. palmata* are rare, and the interlocking framework, diagnostic of the high-density, shallow water, reef crest facies is absent [*Lighty et al.*, 1982] nor are they commonly found occupying the fore reef zone or coral head zone in numerous road cuts on Barbados [*Mesolella*, 1967]. The thick successions of *A. palmata* recovered from drill cores and exploited in this and previous Barbados sea level studies [*Mesolella*, 1967; *Fairbanks*, 1989] provide support that coral samples in this study unambiguously represent the shallow water interlocking framework of the reef crest facies (Figure S1). Hence, our a priori strategy to target the drowned reef crest *A. palmata* for sea level reconstruction is based on arguably the finest sea level indicator species.

3. Results

3.1. The Updated *A. palmata* Sea Level Record 13.9 to 9 kyr B.P.

The Barbados relative sea level reconstruction presented herein consists of 90 individually U-Th-dated *A. palmata* samples (see Text S1) obtained from six offshore drill cores and spans the interval from the mid-Allerød to the earliest Holocene (13.9 kyr to 9 kyr B.P.) (Figure 1a and Table S2). Although 14 *A. palmata* age reversals can be identified within drill cores, after accounting for combined dating uncertainties, depth of *A. palmata* reef crest habitat (+5 m), and drill depth uncertainties (±1 m), all samples can be placed in stratigraphic order (Figure 1a and Table S2). Importantly, throughout the record *A. palmata* samples of similar age plot within 1 to 5 m of each other, strongly supporting that drilling successfully captured the shallow reef crest facies (Figure 1a). This is, perhaps, the most convincing evidence to date to confirm the restricted depth habitat of the *A. palmata* reef crest facies.

3.2. The Barbados Relative Sea Level Curve

In fitting the sea level curve, the shallowest *A. palmata* were assumed to be living closer to the sea surface than those plotting deeper and are used as guide points to generate a "best fit" curve. This takes advantage of the benefits of multiple overlapping cores from multiple expeditions from multiple locations on the south west coast of Barbados. When considering the placement of the best fit curve, we kept within the assumed maximum depth habitat of the *A. palmata* reef crest facies (5 m) without excluding any samples. To better estimate the uncertainty in the placement of our sea level curve relative to the *A. palmata* data and using the simple principle of exclusion, we generated three hypothetical envelopes of uncertainty at +2, +4, and +6 m relative to the Barbados sea level curve (Figure 2). Adding 6 m to the sea level curve unreasonably excludes 91% of the data from living within the prescribed reef crest depth habitat. Adding an uncertainty

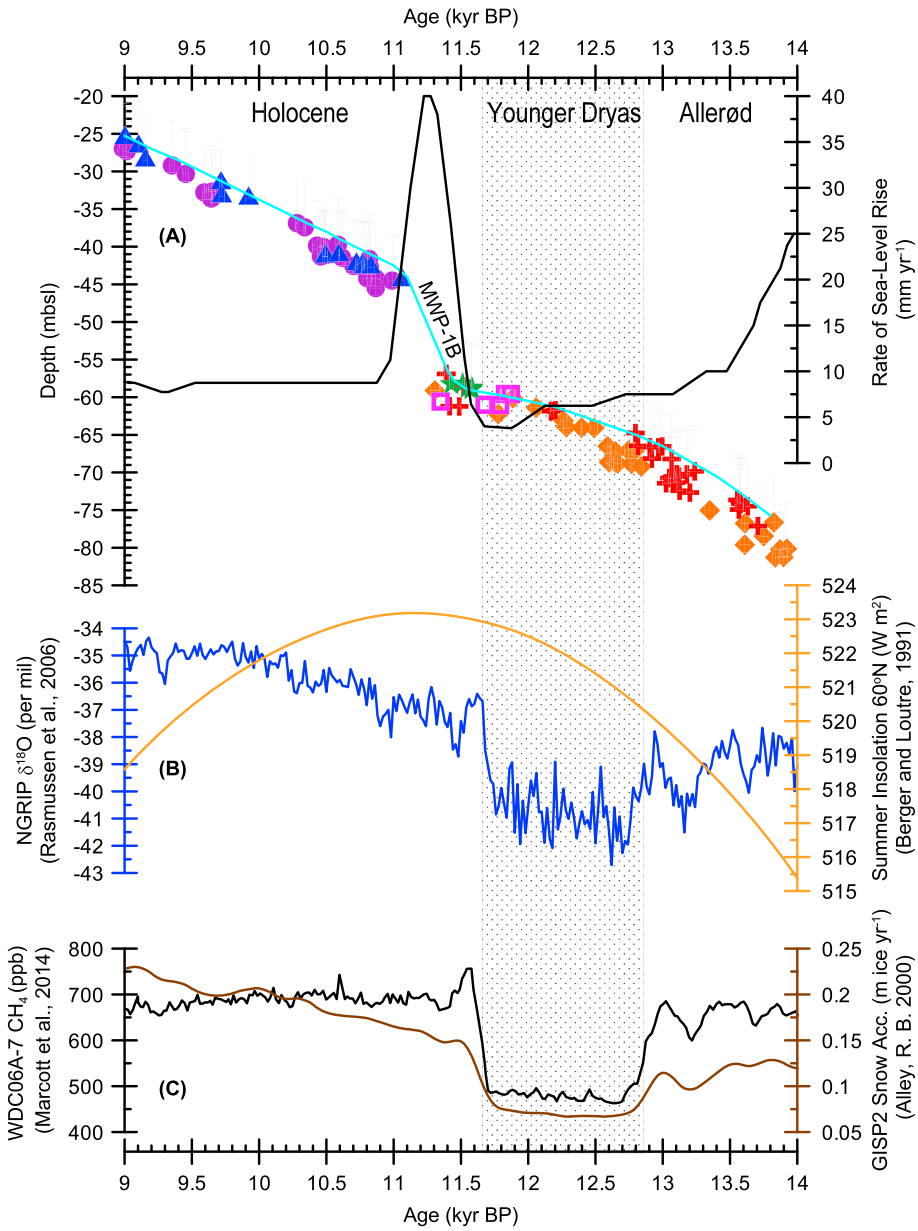

Figure 1. Barbados sea level reconstruction (13.9 to 9 kyr B.P.). (a) Barbados U-Th-dated *Acropora palmata* sea level reconstruction from the mid-Allerød to the early Holocene (13.9 to 9 kyr B.P.). Samples are coded by drill core locations —RGF 7: Blue triangles; RGF 8: Purple circles; RGF 12: Red crosses; RGF 16: Green stars; BBDS 9: Magenta squares; and BBDS 10: Orange diamonds (Figure S1). Ages are reported in thousands of years before present (kyr B.P. relative to 1950). Horizontal error bars in kyr B.P. are age uncertainties reported to 1 sigma (typically smaller than the size of the data point). Depths are reported in meters below present day sea level (mbsl) and are corrected for Barbados' tectonic uplift of 0.34 mm per year (mm yr^{-1}). Vertical lines are + 5 m for *A. palmata*'s depth of habitat uncertainty and ± 1 m for drill depth uncertainty. The cyan line is our estimate of sea level fitted through the *A. palmata* data. The rate of sea level rise curve (black line) in mm yr^{-1} calculated from the Barbados sea level curve (right axis). The stippled rectangle highlights the Younger Dryas Chronozone (12.85 to 11.65 kyr B.P.). All coral data are listed in Table S2. (b) North Greenland Ice Core Project (NGRIP) $\delta^{18}O$ (the blue line) plotted on the GICC05 time scale [*Rasmussen et al.*, 2006] (left axis). The solid orange line represents Summer Insolation at 60°N reported in W m^{-2} [*Berger and Loutre*, 1991] (right axis). (c) West Antarctica Ice Sheet Divide ice core atmospheric CH_4 concentrations (black line) in ppb [*Marcott et al.*, 2014] (left axis) and snow accumulation rates (brown line) in m ice yr^{-1} [*Alley*, 2000] (right axis).

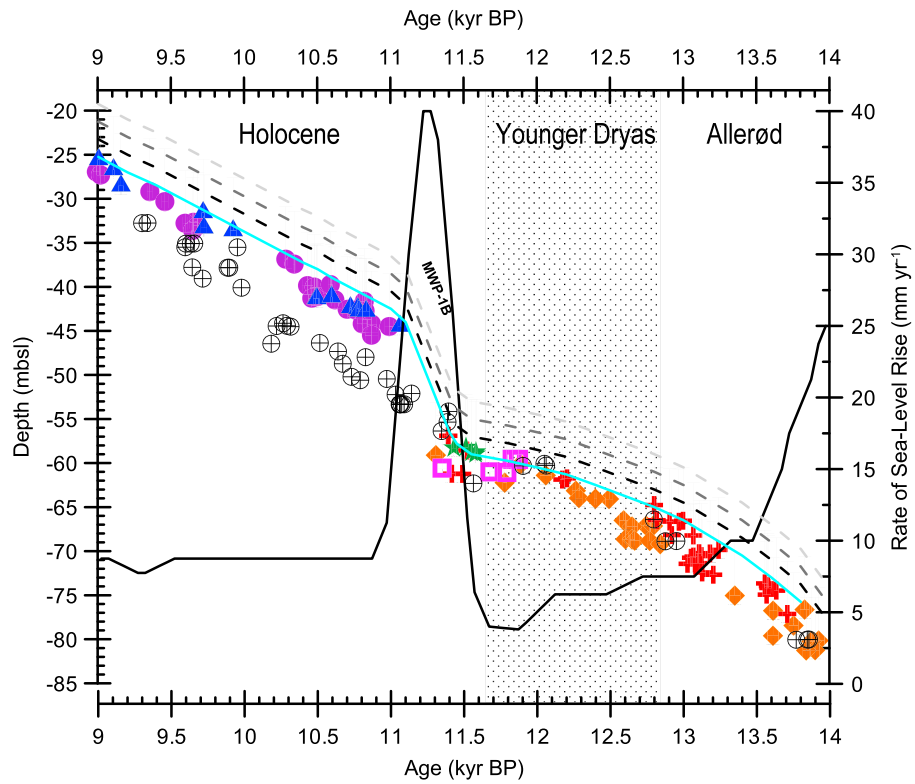

Figure 2. Comparison of Barbados and Tahiti relative sea level reconstructions 13.9–9 kyr B.P. Barbados U-Th-dated *Acropora palmata* sea level reconstruction from the mid-Allerød to the early Holocene (13.9 to 9 kyr B.P.). Samples, age, and depth uncertainties as in Figure 1. The Barbados rate of sea level rise (black line) as in Figure 1. Dashed grey lines (parallel to blue Barbados sea level curve) at +4 and +6 m to the Barbados relative sea level curve represent the uncertainty estimates associated with the reconstruction (see text). Sold black line (parallel to sea level) represents the +2 m best estimate of uncertainty in this study. Also shown are coralgal data used to construct the Tahiti sea level record [*Bard et al.*, 2010]. Plotted data consist of the shallow water coralgal assemblages representing *Acropora danai*, *A. gpe robusta/danai*, *Acropora* sp., *Montastrea annuligera*, and *P. cf verrucosa* with *Pocillopora* sp. (open grey circles) assumed to have a depth restriction of about +6 m (errors not shown).

of +4 m to the sea level curve suggests that 59% of the *A. palmata* were in violation of the 5 m depth restriction. Adding an uncertainty of + 2 m to the Barbados relative sea level curve accommodates 100% of the data suggesting that our hand-drawn curve constrained by an uncertainty of + 2 m provides a reasonable estimate of uncertainty about the Barbados sea level curve. The rate of sea level rise curve was generated by calculating the first derivative (i.e., rate of change) of the sea level curve at 50 year intervals and applying a five-point boxcar average (Figures 1 and 2).

From the mid-Allerød (13.9 kyr B.P.) to the base of MWP-1B (~11.45 kyr B.P.), Barbados *A. palmata* corals record a total sea level rise of ~ 22 m. During this interval, the rate of rise decreased smoothly from about 20 mm yr^{-1} to 4 mm yr^{-1} (Figure 1a). In *Fairbanks* [1989], the Younger Dryas was constrained with four radiocarbon-dated *A. palmata* samples, all contained in a single core. The Younger Dryas interval presented here is now constrained with 19 U-Th-dated *A. palmata* samples from three cores that record 6 m of sea level rise (65 to 59 m below sea level; mbsl) (Figures 1a and 1b). Our computation of the meltwater discharge curve suggests that at the onset of the Younger Dryas, sea level rose at a rate of ~ 7 mm yr^{-1} but had decreased into a "slow stand," by the end of the Younger Dryas with rates of $<$ 4 mm yr^{-1}. Rates of sea level rise rapidly accelerated after 11.45 kyr B.P. producing MWP-1B (Figures 1a and 2). Following the termination of MWP-1B, an *A. palmata* reef crest was reestablished shoreward on a newly flooded carbonate shelf at 11.1 kyr B.P. as indicated by the return of abundant Holocene *A. palmata* samples contained in RGF 7 and 8 samples (Figures 1 and S1). From 11.1 to 9 kyr B.P., *A. palmata* recorded an additional 20 m of sea level rise (47 to 25 mbsl) with rates decreasing from ~ 15 mm yr^{-1} immediately following MWP-1B to ~ 8 mm yr^{-1} by the end of the record presented herein (9 kyr B.P.).

3.3. MWP-1B—Evidence From Barbados Core Lithology for Timing and Amplitude

Two deglacial MWPs were identified at Barbados [*Fairbanks*, 1989]. Whereas MWP-1A was identified at Sunda Shelf [*Hanebuth et al.*, 2000] and Tahiti [*Deschamps et al.*, 2012], MWP-1B was not captured in Tahiti bore hole cores [e.g., *Bard et al.*, 2010], leading to controversy over its authenticity as a feature of the post-Younger Dryas global sea level record [*Lambeck et al.*, 2014]. MWP-1B was first identified and defined as a 15 m jump in the Barbados sea level curve centered at 9500 ^{14}C yr B.P. (11.3 kyr B.P.), based on dated corals from two cores [*Fairbanks,* 1989, 1990]. U-Th-dated *A. palmata* data in six cores now confirm and better constrain the amplitude and timing of MWP-1B as a 14 ± 2 m jump (Figure S2), occurring between 11.45 and 11.1 kyr B.P. with maximum rates of sea level rise approaching 40 mm yr^{-1} (Figure 1a).

4. Discussion

4.1. MWP-1B and Tectonics at Barbados—Uniform Versus Variable Uplift Rates

Sea level records constructed with corals from uplifted reef terraces such as Papua New Guinea [*Edwards et al.*, 1993] and Vanuatu [*Cabioch et al.*, 2003] have insufficient sample resolution to identify the sea level jump associated with MWP-1B at Barbados. Tahiti provides a higher-resolution relative sea level reconstruction for the time period in question; however, the absence of MWP-1B in that record has led *Bard et al.* [2010] to conclude that MWP-1B is an artifact, attributable to accelerated uplift rates at Barbados between the shallow core locations that define the top of MWP-1B (RGF 7 and RGF 8) compared to the deeper core locations defining the base (RGF 12 and RGF 16). In their argument, *Bard et al.* [2010] referred to an onshore SE trending fault absent in outcrop but identified by "offsets in otherwise continuous reef terraces and by abrupt variations in the thickness of the coral cap that are encountered in drill holes" [*Taylor and Mann*, 1991] and suggests that it extends to the shallow offshore drill sites, thus placing the post-MWP-1B core locations in different tectonic environments relative to the deeper core locations that define the base of MWP-1B.

The average uplift rate for the south coast of Barbados and applied to samples in this study is 0.34 mm yr^{-1} based on the elevation of the last interglacial highstand reef [*Broecker et al.*, 1968; *Matthews*, 1973; *Bender et al.*, 1979; *Fairbanks*, 1989]; thus, the difference in uplift correction between 13.9 and 9 yr^{-1} BP age samples is ~ 1.7 m, or negligible. Even a doubling or halving of the average uplift rate would have little impact on our conclusions. For comparison, Tahiti's subsidence rate is estimated to be between 0.39 mm yr^{-1} [*Thomas et al.*, 2012] and 0.15 mm yr^{-1} [*Pirazzoli and Montaggioni*, 1988].

Neither topographic mapping nor multibeam bathymetry provides evidence of an offshore extension of an onshore fault or episodic vertical movement that is restricted to location of the shallow core sites as proposed by *Bard et al.* [2010]. First High Cliff (the last interglacial highstand coral terrace ~ 125 kyr B.P.) runs approximately parallel to the Barbados coastline and varies in elevation between 37 and 41 m in the vicinity of Oisten's Bay and the location of all drill sites. This section of coastline exhibits neither remarkable evidence of displacement, warping, nor a fault zone to mark the location of episodic deformation as argued by *Schellmann and Radtke* [2004].

Stratigraphically, MWP-1B is bracketed by *A. palmata* in deeper and shallower cores and with the termination captured by *A. palmata* overlaying an unconformity representing a lowstand relic Marine Isotope Stage 4 reef (Figure S2). Two samples, RGF 7-27-6 and RGF 8-25-2, immediately below the Holocene *A. palmata* succession were dated at 57.74 ± 0.04 and 64.21 ± 0.42 kyr B.P. (1 sigma), respectively, and have $\delta^{234}U_{initial}$ close to modern values suggesting "closed-system" behavior (Figure S2 and Table S2). We note that MWP-1A similarly represents a break in the Barbados sea level curve, bracketed by deeper and shallower cores with the post-MWP-1A *A. palmata* reestablished on an unconformity consisting of a lowstand ~ 30 kyr relic reef [*Fairbanks*, 1989; *Peltier and Fairbanks*, 2006].

At the base of MWP-1B and at the top of the *A palmata* facies beginning at 53 to 55 mbsl (uncorrected) there is a transition to an 8 to 10 m depth interval of assorted coral rubble primarily consisting of altered fragments of *A. cervicornis* and occasional encrusted and bioeroded fragments of *M. annularis*, *M. cavernosa*, *Diploria* spp., and branching *Porites* spp., fused with carbonate sands, calcareous algae, and reef gravel by calcite cements. This interval is void of the *A. palmata* successions that dominated the mid-Allerød and Younger Dryas. The absence of *A. palmata* reef crest facies within the drill depth interval corresponding to MWP-1B and its succession post-MWP-1B is a consequence of the restricted depth range of the *A. palmata* reef crest

facies and its response to accelerations in the rate of sea level rise. Episodes of sea level rise exceeding the maximum accretion rate of the *A. palmata* reef crest facies cannot be captured in a single core as the inability of the *A. palmata* reef crest to buffer against accelerations in the rate of sea level rise necessitates reestablishment of the facies to shallower waters as observed with MWP-1A [*Fairbanks*, 1989].

4.2. Tahiti Coralgal Assemblages and Their Response to Meltwater Pulses

The Pacific Ocean has no analog for the Atlantic Ocean's reef crest *A. palmata* and sea level estimates are made using the local multispecies coralgal assemblages with variable depth ranges. This deviation from a monospecies sea level reconstruction violates the primary canon on which the Barbados sea level reconstruction is based. As described by *Deschamps et al.* [2012], coralgal assemblages consists of branching and massive corals, encrusting coralline algae, and microbialite communities defined as "organosedimentary deposits" [*Burne and Moore*, 1987]. These microbial communities (up to 80% volume) bind and assimilate detrital material into a carbonate crust [*Heindel et al.*, 2009], are capable of thriving at depths from the sea surface to 25 m, significantly contribute to overall reef accretion [*Pringault et al.*, 2004], and potentially buffers against "reef drowning" during periods of accelerated sea level rise. Barbados' reefs are not devoid of microbialite communities; however, they are most prolific in calmer, deeper waters with reduced turbulence and illumination (10 to 20 mbsl) and on dead coral substrates [*Martindale*, 1992]. These environments are far removed from the shallow high-energy reef crest facies where interlocking *A. palmata* finds its niche.

Bard et al. [2010] present a relative sea level reconstruction for the interval 14 to 9 kyr B.P. using the Pacific Ocean coralgal assemblages of Tahiti with an assigned depth uncertainty of 6 m. It should be noted at Tahiti's neighboring Moorea Island that these "shallow water assemblages" are found thriving on both the barrier reef flat as well as on the outer reef slope in waters 0 to 10 m [*Bouchon*, 1985]. In fitting a line to the Tahiti data, *Bard et al.* [2010] subdivided the Allerød through preboreal climate intervals into three periods of sea level rise to describe average change of rise prior to, during, and following the Younger Dryas. Only five samples from the shallow water assemblage constrain sea level at Tahiti during the 1300 year the Younger Dryas interval (Figure 2). We argue that this section of the Tahiti reconstruction lacks the resolution and their shallow water reef assemblage lack the restricted depth of necessary to constrain nonlinearity in the sea level record modulated by the relationships between climate change and ice sheet dynamics [*Lambeck et al.*, 2002; *Stanford et al.*, 2006; *McNeall et al.*, 2011; *Lenton et al.*, 2012]. By contrast, the water depth restriction of the Barbados *A. palmata* reef crest facies makes it a less ambiguous sea level indicator, and the higher-resolution Barbados *A. palmata* sea level record illustrates the systematic response of sea level to the Younger Dryas climate reversal, the readvance of glaciers, and their rapid demise coincident with the insolation maximum at 60°N.

It is significant that we identified a slow stand in the latter half of the Younger Dryas that persisted until ~ 11.45 kyr B.P. This deceleration and subsequent acceleration in ice sheet melting during MWP-1B are entirely consistent with terrestrial data of climate and ice sheet changes and suggest that the sawtooth characteristics of large ice sheets (growing slower than they melt) as determined by *Broecker and van Donk* [1970] and *Hays et al.* [1976] can prevail on time scales much shorter than the orbital cycles

The imposition of the Younger Dryas stadial onto the deglaciation altered the relationship between glacial melting and insolation forcing creating a state of disequilibrium that persisted for ~ 1300 years. By the end of the Younger Dryas, the forcing(s) that produced and maintained glacial-like conditions in the circum-North Atlantic quickly abated at a time when Northern Hemisphere insolation was near its peak, requiring a rapid readjustment in the Northern Hemisphere ice sheets. Newly regenerated and thermally unstable ice sheets, particularly when formed in lower latitude temperate regions (40°N to 45°N), are more responsive to insolation forcing [*Abe-Ouchi et al.*, 2013]. The acceleration in the rate of sea level rise associated with MWP-1B and the rapid recovery of any sea level deficit created by the Younger Dryas sea level slow stand served to place ice sheets and hence sea level back into equilibrium with insolation forcing. In essence, the occurrence of the Younger Dryas sea level slow stand tied to the North Atlantic regional climate reversal predicts and requires that a MWP follow.

4.3. The Barbados Sea Level Record and the Younger Dryas Cold Snap in Context

The Barbados sea level record chronicles 6 m of sea level rise with rates of rise that slowed in the mid-Allerød and through the Younger Dryas and thus excludes a jump in sea level to trigger the Younger Dryas. In the discussion to follow, we distance ourselves from catastrophic oceanic triggers and revisit Younger Dryas cooling in terms of shifting air masses and variable wind strengths responding to the changing geometries

of a deglaciating North American landscape that was closely coupled to the atmosphere [*Manabe and Broccoli*, 1985; *Boulton and Clark*, 1990; *Wunsch*, 1998; *Ullman et al*., 2014].

General circulation models show that the δ^{18}O of Greenland ice is not only correlated with temperature but is controlled by the relative contributions of Atlantic versus Pacific sourced water vapor [*Craig*, 1961; *Charles et al*., 1994]. Furthermore, *Liu et al*. [2012] contend that the changing ice sheet topography reconfigured atmospheric circulation during the Younger Dryas, thereby altering the δ^{18}O—temperature air mass mixing relationship. These studies demonstrate that δ^{18}O variations and accumulation patterns in Greenland ice cores respond to changes in atmospheric fronts, regional air masses, and sea ice dynamics; therefore, "abrupt" shifts associated with the Younger Dryas need not be interpreted solely in terms of low to high-latitude energy balance changes but can simply reflect local changes over Greenland in response to changing air mass mixing ratios.

At the LGM the Laurentide ice sheet is modeled to have sequestered 25 to 35 million km^3 of ice [*Denton and Hughes*, 1981], or equivalent to a 72 to 100 m lowering in sea level [*Ruddiman*, 2001]. Its highest ice dome(s) added 3000 m of elevation to the northeastern sectors of the North American continent altering atmospheric circulation patterns over North America, Europe, and Greenland [*Manabe and Broccoli*, 1985]. Models simulate a bifurcated North American Jet Stream that flowed around Laurentide's perimeter and a North Atlantic polar front located south of 45°N [*Ruddiman and McIntyre*, 1981; *Rind et al*., 1986; *Cooperative Holocene Mapping Project*, 1988; *Keigwin and Lehman*, 1994] that confined comparatively warmer and wetter conditions to the south and west of the ice sheet and cooler dryer conditions to the north. Paleoclimate reconstructions infer extensive permanent North Atlantic winter sea ice cover that compressed the storm track between the southernmost sea ice margin and the northernmost boundary of the Laurentide ice sheet, starving much of the interior of the Laurentide, Arctic, and Fennoscandian ice sheets of winter precipitation [*Ruddiman and McIntyre*, 1981].

By the onset of the Younger Dryas and approaching the midpoint of deglaciation, sea level had risen by ~ 50 m [*Fairbanks*, 1989; *Peltier and Fairbanks*, 2006]. The reduction in the overall size and change in topography of the North American ice sheets undoubtedly influenced the steering of the jet stream, the strength of the westerlies, and the delivery of moisture to the North Atlantic and Europe. A readvance in the North Atlantic Polar Front and sea ice boundaries [*Ruddiman and McIntyre*, 1981; *de Vernal and Hillaire-Marcel*, 2000] as recorded by peak abundances of subpolar planktonic foraminifera morphotypes [*Ruddiman and McIntyre*, 1981; *Bond et al*., 1997] and sea ice regeneration in the Arctic and northern Norway all suggest a much cooler North Atlantic [*Stein and Fahl*, 2012; *Cabedo-Sanz et al*., 2013]. The role of sea ice is particularly important to density-driven circulation [*Dyke*, 2004] and albedo-based cooling (positive feedbacks associated with an amplification of seasonality [*Denton et al*., 2005] and insulation of the ocean's heat from the atmosphere [*Lenton et al*., 2008]), which negatively impacts the atmosphere's ability to hold and deliver moisture to continental ice sheets [*Alley et al*., 1993] while simultaneously changing atmospheric circulation patterns and displacing conventional pathways of moisture delivery.

We suggest focused moisture delivery by the North American Jet Stream promoted ice sheet resurgence in the Fennoscandian region during the Younger Dryas [*Winguth et al*., 2005; *Cuffey and Paterson*, 2010] as recorded in lower equilibrium line altitudes in Norway [*Larsen and Stalsberg*, 2004] and early cessation of retreat and ice sheet readvances in some areas of Fennoscandinavia [*Andersen et al*., 1995]. The Younger Dryas sea level response, observed as a slowdown, matches the expected global ice volume response to an advancement of the Fennoscandian ice sheet in combination with reduced melting of the Laurentide and Greenland ice sheets.

While no single record provides irrefutable evidence for a large-scale readvance in the Fennoscandian ice sheet during the Younger Dryas, the volumetric change in ice necessary to generate the sea level response (Figure 1a) need not eliminate it from consideration. The Fennoscandian ice sheet at its LGM maximum is estimated to have contained ~7.3 million km^3 of ice [*Denton and Hughes*, 1981]. Had the rate of sea level rise at Barbados increased uniformly at the rates observed from 13.9 to 13 kyr B.P., sea level would be predicted to have been higher by about 8 m by the end of the Younger Dryas (i.e., 50 rather than 58 mbsl). Therefore, reconciliation of an ~ 8 m "sea level deficit" (2.9 million km^3 ice volume equivalent) can be achieved by the focused regeneration of the Fennoscandian ice sheet [e.g., *Winguth et al*., 2005] in conjunction with reduced Laurentide and Greenland melting.

By the latter part of the Younger Dryas, the progressive thinning and retreat of the Laurentide ice sheet potentially allowed a repositioning of the North American Jet Stream to the north [*Manabe and Broccoli*, 1985] which was accompanied by a northward retreat of the polar front, increased variability of the sea ice boundaries [*Ruddiman and McIntyre*, 1981; *Pearce et al*., 2014] and possibly the gradual recovery of the NADW overturning [*McManus et al*., 2004]. Moisture transport shifted toward Greenland, via conventional North American and North Atlantic routes and sources including potentially ice-free Norwegian and Greenland Seas [*Charles et al*., 1994; *Cabedo-Sanz et al*., 2013], marked by increased snow accumulation rates [*Alley et al*., 1993] and recorded imprinted on the Greenland ice core records (Figure 1c). In contrast, the Fennoscandian ice sheet, now removed from the storm track, may have become starved for moisture. Westerly winds blowing over a repositioned Gulf Stream and North Atlantic Drift channeled warm air toward the Fennoscandian region [*Seager et al*., 2002], ablation exceeded snow accumulation, and deglaciation of the Northern Hemisphere ice sheets resumed in earnest. Surface hydrofracturing [e.g., *Scambos et al*., 2009] and resumption of rapid sea level rise, as recorded at Barbados beginning around 11.45 kyr B.P., may also have provided positive feedback accelerating the destabilization of ice shelves and promoting calving and undermining of grounded glaciers.

Although we have attributed the resumption of sea level rise following the termination of the Younger Dryas to melting of Northern Hemisphere ice sheets, we cannot completely discount an Antarctic contribution to MWP-1B and the post-MWP-1B Barbados sea level record. After nearly 50 years of study the history of deglaciation at Antarctica remains unresolved, and the complexities of GIA models and their predictions for fingerprinting MWPs are still being refined [*Hay et al*., 2014]. Modelers and glaciologists [*Peltier*, 2004; *Mackintosh et al*., 2011] continue to revisit an Antarctic contribution to MWP-1B although geological evidence for deglaciation is sparse, localized, poorly constrained chronologically [*Okuno and Miura*, 2013], and geographically restricted along individual ice streams and mass conservative with ice flowing from east to west Antarctica and little evidence of a net loss [*Bentley et al*., 2014]. If a Southern Hemisphere source contributed significantly to MWP-1A as argued by *Clark et al.* [2002], *Weaver et al.* [2003], and *Deschamps et al.* [2012], the AIS likely had insufficient ice volume at the end of the Younger Dryas to have contributed more than a few meters to the amplitude of MWP-1B.

5. Conclusions

The rate of sea level rise following MWP-1A decreased smoothly through the Allerød culminating in the "Younger Dryas slow stand" before reaccelerating into MWP-1B beginning at 11.45 kyr B.P. The Barbados sea level reconstruction excludes a measurable meltwater pulse as a trigger for the Younger Dryas and records a rise of 6 m decreasing in rate from 7 mm yr^{-1} at the start to a slow stand of 4 mm yr^{-1} by the end. The decrease in the rate of sea level rise is quite possibly a fingerprint for the advancement of the Fennoscandian Ice Sheet. We interpret the main pulse of melting defining MWP-1B (centered at 11.3 kyr B.P.) as the delayed response of Northern Hemisphere ice sheets to the northward retreat of the polar front and marking the termination of the climatic imprint made by the Younger Dryas Chronozone. MWP-1B lagged the end of the Younger Dryas and the increase in $\delta^{18}O$ and snow accumulation rates measured in the NGRIP ice core record by about 400 years and is entirely consistent with the ice sheet response, and hence sea level, to abrupt atmospheric shifts based on glacial equilibrium models. Maximum Northern Hemisphere summer insolation coupled with a reintensification of North Atlantic overturning fueled ice sheet disintegration, culminating in MWP-1B here confirmed as a 14 ± 2 m sea level jump at Barbados with rates approaching 40 mm yr^{-1} (Figure 1a). Rapid melting may have been amplified by greenhouse gas warming from elevated atmospheric CO_2 and CH_4 (Figure 1c) although the magnitude of CO_2 and CH_4 change is less than one third of the change in these gases in the past century [e.g., *Intergovernmental Panel on Climate Change*, 2013]. Following the termination of MWP-1B (11.1 kyr B.P.), the rate of Holocene sea level rise decreased smoothly in a manner similar to post-MWP-1A.

The balance between insolation forcing and ice sheet melting during deglaciation can be disrupted by various mechanisms. When the ice sheet is out of equilibrium with climate forcing, the rate of melting must adjust and is measured by the rate of sea level rise. The significant decrease in global ice sheet melting during the Younger Dryas requires a more rapid rate of melting once the Younger Dryas forcing is removed. Thus, a MWP following the Younger Dryas is predicted and required because the ice sheets at the end of the Younger Dryas were out of equilibrium.

Atmospheric modeling studies in the 1970's and 1980's concluded that the cause(s) of the Younger Dryas climate event centered on atmospheric forcing driven by changing geometries of the Northern Hemisphere ice sheet lobes. Subsequent ice core results from Greenland found evidence that the onset and termination of the Younger Dryas climate event took place over several decades adding strong support for an atmospheric mechanism. This work was followed by more than two decades of intense research by the marine paleoceanography community that pursued evidence for the catastrophic shutdown of NADW initiating the Younger Dryas event. Neither evidence for a shutdown of NADW nor a catastrophic MWP to trigger a shutdown has been found, and proponents of the original flood hypothesis have themselves stepped back from originally proposed catastrophic origins for the Younger Dryas cold snap [*Broecker et al*., 2010]. Rather than catastrophic triggers, it is the complex interaction between oceanic and atmospheric coupling along with insolation forcing that may determine the occurrence of Younger Dryas—Bølling Allerød warm-cold oscillations during deglaciations [*Cheng et al*., 2006; *Carlson*, 2008; *Renssen et al*., 2015]. Our sea level data tilt the balance of evidence back to the original atmospheric models and the role of changing Jet Stream geometries combined with sea ice distribution as the most probable cause of the Younger Dryas climate event and suggest that any reductions in the AMOC, interpreted in deep-sea core records during the Younger Dryas, were a response to shifting atmospheric fronts, sea ice distribution, and wind patterns and intensities. Therefore, the Younger Dryas abrupt cold event may not be relevant to the future global warming scenarios that frequently cite the dire consequences of a meltwater-induced shutdown in NADW formation.

Acknowledgments
We are grateful to the Captain and Crew of the R/V *Ranger* 88-13 and R/V *Knorr* 189-2, Fugro McClelland, and Warren George Drilling Inc. Thanks to L. Cao, K. Ellins, L. Teneva, J. Mey, T. Emge, A. Cotet, and C. Vidito for their technical contributions to this manuscript. We appreciate the insightful discussions and constructive comments from K. Miller and A. Broccoli (Rutgers University) and from an anonymous reviewer. This research was made possible by the National Science Foundation grants (OCE09-28446 and OCE05-50900), The School of Arts and Sciences and The Department of Earth and Planetary Sciences Rutgers University, New Brunswick, Rutgers University, and the William H. Greenberg Fellowship via the Climate and Environmental Change Initiative (Rutgers/Phyllis Greenberg). New data presented herein are available in the supporting information and will be archived on the web at http://geology.rutgers.edu/recent-publications.

References

Aagaard, K., and E. C. Carmack (1989), The role of sea ice and other fresh water in the Arctic circulation, *J. Geophys. Res.*, *94*, 14,485–14,498.
Abe-Ouchi, A., F. Saito, K. Kawamura, M. E. Raymo, J. Okuno, K. Takahashi, and H. Blatter (2013), Insolation-driven 100,000-year glacial cycles and hysteresis of ice-sheet volume, *Nature*, *500*(7461), 190–193.
Alley, R. (2000), The Younger Dryas cold interval as viewed from central Greenland, *Quat. Sci. Rev.*, *19*(1–5), 213–226.
Alley, R., et al. (1993), Abrupt increase in Greenland snow accumulation at the end of the Younger Dryas event, *Nature*, *362*(6420), 527–529.
Andersen, B. G., J. Lundqvist, and M. Saarnisto (1995), The Younger Dryas margin of the Scandinavian Ice Sheet—An introduction, *Quat. Int.*, *28*, 145–146.
Austermann, J., J. X. Mitrovica, K. Latychev, and G. A. Milne (2013), Barbados-based estimate of ice volume at Last Glacial Maximum affected by subducted plate, *Nat. Geosci.*, *6*, 553–557.
Bard, E., B. Hamelin, and R. G. Fairbanks (1990), U-Th ages obtained by mass spectrometry in corals from Barbados: Sea level during the past 130,000 years, *Nature*, *346*(6283), 456–458.
Bard, E., B. Hamelin, and D. Delanghe-Sabatier (2010), Deglacial meltwater pulse 1B and Younger Dryas sea levels revisited with boreholes at Tahiti, *Science*, *327*(5970), 1235–1237.
Bassett, S. E., G. A. Milne, J. X. Mitrovica, and P. U. Clark (2005), Ice sheet and solid earth influences on far-field sea-level histories, *Science*, *309*(5736), 925–928.
Bender, M., R. G. Fairbanks, F. W. Taylor, R. K. Matthews, E. A. Goddard, and W. Broecker (1979), Uranium-series dating of the Pleistocene reef tracts of Barbados, West Indies, *Geol. Soc. Am. Bull.*, *90*(6), 577–594.
Bentley, M. J., et al. (2014), A community-based geological reconstruction of Antarctic Ice Sheet deglaciation since the Last Glacial Maximum, *Quat. Sci. Rev.*, *100*, 1–9.
Berger, A., and M. F. Loutre (1991), Insolation values for the climate of the last 10 million years, *Quat. Sci. Rev.*, *10*(4), 297–317.
Björck, S. (2007), Younger Dryas oscillation, global evidence. 1987–1994, in *Encyclopedia of Quaternary Science*, vol. 3, edited by S. A. Elias, pp. 1985–1993, Elsevier, Oxford, U. K.
Björck, S., et al. (1996), Synchronized terrestrial atmospheric deglacial records around the North Atlantic, *Science*, *274*(5290), 1155–1160.
Bond, G., et al. (1992), Evidence for massive discharges of icebergs into the North Atlantic Ocean during the last glacial period, *Nature*, *360*, 245–249.
Bond, G., W. Showers, M. Cheseby, R. Lotti, P. Almasi, P. deMenocal, P. Priore, H. Cullen, I. Hajdas, and G. Bonani (1997), A pervasive millennial-scale cycle in North Atlantic Holocene and glacial climates, *Science*, *278*(5341), 1257–1266.
Bouchon, C. (1985), Quantitative study of Scleractinian Coral communities of Tiahura Reef (Moorea Island, French Polynesia), in *Proceedings of the Fifth International Coral Reef Congress*, vol. 6, pp. 279–284, Tahiti.
Boulton, G. S., and C. D. Clark (1990), A highly mobile Laurentide ice sheet revealed by satellite images of glacial lineations, *Nature*, *346*(6287), 813–817.
Boulton, G. S., P. Dongelmans, M. Punkari, and M. Broadgate (2001), Palaeoglaciology of an ice sheet through a glacial cycle: The European ice sheet through the Weichselian, *Quat. Sci. Rev.*, *20*(4), 591–625.
Brauer, A., C. Endres, C. Günter, T. Litt, M. Stebich, and J. F. W. Negendank (1999), High resolution sediment and vegetation responses to Younger Dryas climate change in varved lake sediments from Meerfelder Maar, Germany, *Quat. Sci. Rev.*, *18*(3), 321–329.
Brauer, A., G. H. Haug, P. Dulski, D. M. Sigman, and J. F. W. Negendank (2008), An abrupt wind shift in western Europe at the onset of the Younger Dryas cold period, *Nat. Geosci.*, *1*(8), 520–523.
Broecker, W., and G. H. Denton (1989), The role of ocean-atmosphere reorganizations in glacial cycles, *Geochim. Cosmochim. Acta*, *53*(10), 2465–2501.
Broecker, W., and J. van Donk (1970), Insolation changes, ice volumes, and the O^{18} record in deep-sea cores, *Rev. Geophys.*, *8*, 169–198.
Broecker, W., D. L. Thurber, J. Goddard, T.-l. Ku, R. K. Matthews, and K. J. Mesolella (1968), Milankovitch hypothesis supported by precise dating of coral reefs and deep-sea sediments, *Science*, *159*(3812), 297–300.
Broecker, W., D. M. Peteet, and D. Rind (1985), Does the ocean-atmosphere system have more than one stable mode of operation?, *Nature*, *315*(6014), 21–26.

Broecker, W., J. P. Kennett, B. P. Flower, J. T. Teller, S. Trumbore, G. Bonani, and W. Wolfli (1989), Routing of meltwater from the Laurentide Ice Sheet during the Younger Dryas cold episode, *Nature*, *341*(6240), 318–321.
Broecker, W., G. H. Denton, R. L. Edwards, H. Cheng, R. B. Alley, and A. E. Putnam (2010), Putting the Younger Dryas cold event into context, *Quat. Sci. Rev.*, *29*(9–10), 1078–1081.
Brook, E., S. Harder, J. Severinghaus, E. J. Steig, and C. M. Sucher (2000), On the origin and timing of rapid changes in atmospheric methane during the last glacial period, *Global Biogeochem. Cycles*, *14*, 559–572.
Burne, R., and L. S. Moore (1987), Microbialites; organosedimentary deposits of benthic microbial communities, *Palaios*, *2*(3), 241–254.
Cabedo-Sanz, P., S. T. Belt, J. Knies, and K. Husum (2013), Identification of contrasting seasonal sea ice conditions during the Younger Dryas, *Quat. Sci. Rev.*, *79*, 74–86.
Cabioch, G., K. A. Banks-Cutler, W. J. Beck, G. S. Burr, T. Corrège, R. Lawrence Edwards, and F. W. Taylor (2003), Continuous reef growth during the last 23 cal kyr BP in a tectonically active zone (Vanuatu, South West Pacific), *Quat. Sci. Rev.*, *22*(15–17), 1771–1786.
Carlson, A. (2008), Why there was not a Younger Dryas-like event during the penultimate deglaciation, *Quat. Sci. Rev.*, *27*(9–10), 882–887.
Carlson, A., and P. Clark (2012), Ice sheet sources of sea level rise and freshwater discharge during the last deglaciation, *Rev. Geophys.*, *50*, RG4007, doi:10.1029/2011RG000371.
Charles, C. D., D. Rind, J. Jouzel, R. D. Koster, and R. G. Fairbanks (1994), Glacial-interglacial changes in moisture sources for Greenland: Influences on the ice core record of climate, *Science*, *263*(5146), 508–511.
Cheng, H., R. L. Edwards, Y. Wang, X. Kong, Y. Ming, M. J. Kelly, X. Wang, C. D. Gallup, and W. Liu (2006), A penultimate glacial monsoon record from Hulu Cave and two-phase glacial terminations, *Geology*, *34*(3), 217–220.
Clark, J. A., W. E. Farrell, and W. R. Peltier (1978), Global changes in postglacial sea level: A numerical calculation, *Quat. Res.*, *9*(3), 265–287.
Clark, P., J. X. Mitrovica, G. A. Milne, and M. E. Tamisiea (2002), Sea-level fingerprinting as a direct test for the source of global meltwater pulse 1A, *Science*, *295*(5564), 2438–2441.
Clark, P., A. S. Dyke, J. D. Shakun, A. E. Carlson, J. Clark, B. Wohlfarth, J. X. Mitrovica, S. W. Hostetler, and A. M. McCabe (2009), The Last Glacial Maximum, *Science*, *325*(5941), 710–714.
CLIMAP Project Members (1981), Seasonal reconstructions of the Earth's surface at the Last Glacial Maximum in Map Series, Tech. Rep. MC-36, Geol. Soc. of Am., Boulder, Colo.
Cooperative Holocene Mapping Project (1988), Climatic changes of the last 18,000 years: Observations and model simulations, *Science*, *241*(4869), 1043–1052.
Condron, A., and P. Winsor (2012), Meltwater routing and the Younger Dryas, *Proc. Natl. Acad. Sci. U.S.A.*, *109*(49), 19,928–19,933.
Craig, H. (1961), Isotopic variations in meteoric waters, *Science*, *133*(3465), 1702–1703.
Cuffey, K., and G. D. Clow (1997), Temperature, accumulation, and ice sheet elevation in central Greenland through the last deglacial transition, *J. Geophys. Res.*, *102*, 26,383–26,396.
Cuffey, K., and W. S. Paterson (2010), *The Physics of Glaciers*, 4th ed., 704 pp., Elsevier, Oxford, U. K.
Cutler, K. B., R. L. Edwards, F. W. Taylor, H. Cheng, J. Adkins, C. D. Gallup, P. M. Cutler, G. S. Burr, and A. L. Bloom (2003), Rapid sea-level fall and deep-ocean temperature change since the last interglacial period, *Earth Planet. Sci. Lett.*, *206*(3–4), 253–271.
Dansgaard, W., et al. (1993), Evidence for general instability of past climate from a 250-kyr ice-core record, *Nature*, *364*(6434), 218–220.
de Vernal, A., and C. Hillaire-Marcel (2000), Sea-ice cover, sea-surface salinity and halo-/thermocline structure of the northwest North Atlantic: Modern versus full glacial conditions, *Quat. Sci. Rev.*, *19*(1–5), 65–85.
de Vernal, A., C. Hillaire-Marcel, and G. Bilodeau (1996), Reduced meltwater outflow from the Laurentide ice margin during the Younger Dryas, *Nature*, *381*(6585), 774–777.
Denton, G., and T. J. Hughes (1981), *The Last Great Ice Sheets*, 484 pp., Wiley, New York.
Denton, G., R. B. Alley, G. C. Comer, and W. S. Broecker (2005), The role of seasonality in abrupt climate change, *Quat. Sci. Rev.*, *24*(10–11), 1159–1182.
Deschamps, P., N. Durand, E. Bard, B. Hamelin, G. Camoin, A. L. Thomas, G. M. Henderson, J. Okuno, and Y. Yokoyama (2012), Ice-sheet collapse and sea-level rise at the Bølling warming 14,600 years ago, *Nature*, *483*(7391), 559–564.
Dyke, A. S. (2004), An outline of North American deglaciation with emphasis on central and northern Canada, in *Developments in Quaternary Sciences*, edited by J. Ehlers and P. L. Gibbard, pp. 373–424, Elsevier, Amsterdam.
Edwards, L., J. W. Beck, G. S. Burr, D. J. Donahue, J. M. A. Chappell, A. L. Bloom, E. R. M. Druffel, and F. W. Taylor (1993), A large drop in atmospheric $^{14}C/^{12}C$ and reduced melting in the Younger Dryas, documented with ^{230}Th ages of corals, *Science*, *260*(5110), 962–968.
Elmore, A. C., and J. D. Wright (2011), North Atlantic deep water and climate variability during the Younger Dryas cold period, *Geology*, *39*, 107–110.
Fairbanks, R. (1989), A 17,000-year glacio-eustatic sea level record: Influence of glacial melting rates on the Younger Dryas event and deep-ocean circulation, *Nature*, *342*(6250), 637–642.
Fairbanks, R. (1990), The age and origin of the "Younger Dryas climate event" in Greenland ice cores, *Paleoceanography*, *5*, 937–948.
Fairbanks, R., C. D. Charles, and J. D. Wright (1992), Origin of global meltwater pulses, in *Radiocarbon After Four Decades: An Interdisciplinary Perspective*, edited by R. E. Taylor, A. A. Long, and R. S. Kra, pp. 473–500, Springer, New York.
Firestone, R. B., et al. (2007), Evidence for an extraterrestrial impact 12,900 years ago that contributed to the megafaunal extinctions and the Younger Dryas cooling, *Proc. Natl. Acad. Sci. U.S.A.*, *104*(41), 16,016–16,021.
Flower, B. P., and J. P. Kennett (1990), The Younger Dryas cool episode in the Gulf of Mexico, *Paleoceanography*, *5*, 949–961.
Flower, B. P., D. W. Hastings, H. W. Hill, and T. M. Quinn (2004), Phasing of deglacial warming and Laurentide Ice Sheet meltwater in the Gulf of Mexico, *Geology*, *32*(7), 597–600.
Gallup, C. D., R. L. Edwards, and R. G. Johnson (1994), The timing of high sea levels over the past 200,000 years, *Science*, *263*(5148), 796–800.
Gallup, C. D., H. Cheng, F. W. Taylor, and R. L. Edwards (2002), Direct determination of the timing of sea level change during Termination II, *Science*, *295*(5553), 310–313.
Gladfelter, E. (1982), Skeletal development in *Acropora cervicornis*. Patterns of calcium carbonate accretion in the axial corallite, *Coral Reefs*, *1*(1), 45–51.
Gladfelter, E., R. K. Monahan, and W. B. Gladfelter (1978), Growth rates of five reef-building corals in the Northeastern Caribbean, *Bull. Mar. Sci.*, *28*(4), 728–734.
Goreau, T. (1959), The ecology of Jamaican Coral Reefs I. Species composition and zonation, *Ecology*, *40*(1), 67–90.
Goreau, T., and J. W. Wells (1967), The shallow-water scleractinia of Jamaica: Revised list of species and their vertical distribution range, *Bull. Mar. Sci.*, *17*(2), 442–453.
Hanebuth, T., K. Stattegger, and P. M. Grootes (2000), Rapid flooding of the Sunda Shelf: A late-glacial sea-level record, *Science*, *288*(5468), 1033–1035.

Hay, C., J. X. Mitrovica, N. Gomez, J. R. Creveling, J. Austermann, and R. E. Kopp (2014), The sea-level fingerprints of ice-sheet collapse during interglacial periods, *Quat. Sci. Rev.*, *87*, 60–69.
Hays, J. D., J. Imbrie, and N. J. Shackleton (1976), Variations in the Earth's orbit: Pacemaker of the Ice Ages, *Science*, *194*(4270), 1121–1132.
Heindel, K., M. A. X. Wisshak, and H. Westphal (2009), Microbioerosion in Tahitian reefs: A record of environmental change during the last deglacial sea-level rise (IODP 310), *Lethaia*, *42*(3), 322–340.
Hubbard, D. (2009), Depth and species-related patterns of Holocene reef accretion in the Caribbean and Western Atlantic: A critical assessment of existing models, in *Perspectives in Carbonate Geology: A Tribute to the Career of Robert Nathan Ginsburg*, *Spec. Publ.*, vol. 41, edited by P. Swart, G. P. Eberli, and J. McKenzie, pp. 1–18, Int. Assoc. Sedimentol.
Intergovernmental Panel on Climate Change (2013), *Summary for Policymakers*, Cambridge Univ. Press, Cambridge, U. K.
Jouzel, J., C. Lorius, J. R. Petit, C. Genthon, N. I. Barkov, V. M. Kotlyakov, and V. M. Petrov (1987), Vostok ice core: A continuous isotope temperature record over the last climatic cycle (160,000 years), *Nature*, *329*(6138), 403–408.
Keigwin, L., and S. J. Lehman (1994), Deep circulation change linked to HEINRICH Event 1 and Younger Dryas in a middepth North Atlantic Core, *Paleoceanography*, *9*, 185–194.
Khatiwala, S. P., R. G. Fairbanks, and R. W. Houghton (1999), Freshwater sources to the coastal ocean off northeastern North America: Evidence from $H_2{}^{18}O/H_2{}^{16}O$, *J. Geophys. Res.*, *104*, 18,241–18,255.
Kleman, J., C. Hättestrand, I. Borgström, and A. P. Stroeven (1997), Fennoscandian paleoglaciology reconstructed using a glacial geological inversion model, *J. Glaciol.*, *43*, 283–299.
Lambeck, K., T. M. Esat, and E.-K. Potter (2002), Links between climate and sea levels for the past three million years, *Nature*, *419*(6903), 199–206.
Lambeck, K., H. Rouby, A. Purcell, Y. Sun, and M. Sambridge (2014), Sea level and global ice volumes from the Last Glacial Maximum to the Holocene, *Proc. Natl. Acad. Sci. U.S.A.*, *111*, 15,296–15,303.
Larsen, E., and M. Stalsberg (2004), Younger Dryas glaciolacustrine rhythmites and cirque glacier variations at Kråkenes, western Norway: Depositional processes and climate, *J. Paleolimnol.*, *31*(1), 49–61.
Lasalle, P., and W. W. Shilts (1993), Younger Dryas-age readvance of Laurentide ice into the Champlain Sea, *Boreas*, *22*(1), 25–37.
Lemdahl, G. (1991), A rapid climatic change at the end of the Younger Dryas in south Sweden—Palaeoclimatic and palaeoenvironmental reconstructions based on fossil insect assemblages, *Palaeogeogr. Palaeoclimatol. Palaeoecol.*, *83*, 313–331.
Lenton, T. M., H. Held, E. Kriegler, J. W. Hall, W. Lucht, S. Rahmstorf, and H. J. Schellnhuber (2008), Tipping elements in the Earth's climate system, *Proc. Natl. Acad. Sci. U.S.A.*, *105*(6), 1786–1793.
Lenton, T. M., V. N. Livina, V. Dakos, and M. Scheffer (2012), Climate bifurcation during the last deglaciation, *Clim. Past Discuss.*, *8*, 321–348.
Lighty, R. G., I. G. Macintyre, and R. Stuckenrath (1982), *Acropora palmata* reef framework: A reliable indicator of sea level in the Western Atlantic for the past 10,000 years, *Coral Reefs*, *1*, 125–130.
Liu, Z., et al. (2012), Younger Dryas cooling and the Greenland climate response to CO_2, *Proc. Natl. Acad. Sci. U.S.A.*, *109*, 11,101–11,104.
Lowell, T., G. J. Larson, J. D. Hughes, and G. H. Denton (1999), Age verification of the Lake Gribben forest bed and the Younger Dryas advance of the Laurentide Ice Sheet, *Can. J. Earth Sci.*, *36*(3), 383–393.
Lowell, T., et al. (2005), Testing the Lake Agassiz meltwater trigger for the Younger Dryas, *Eos Trans. AGU*, *86*(40), 365–373.
Mackintosh, A., et al. (2011), Retreat of the East Antarctic ice sheet during the last glacial termination, *Nat. Geosci.*, *4*(3), 195–202.
Manabe, S., and A. J. Broccoli (1985), The influence of continental ice sheets on the climate of an ice age, *J. Geophys. Res.*, *90*, 2167–2190.
Mangerud, J., S. Anderson, B. Berglund, and J. Donner (1974), Quaternary stratigraphy of Norden, a proposal for terminology and classification, *Boreas*, *3*, 109–128.
Marcott, S. A., et al. (2014), Centennial-scale changes in the global carbon cycle during the last deglaciation, *Nature*, *514*(7524), 616–619.
Martindale, W. (1992), Calcified epibionts as palaeoecological tools: Examples from the recent and Pleistocene reefs of Barbados, *Coral Reefs*, *11*(3), 167–177.
Matthews, R. K. (1972), Dynamics of the ocean-cryosphere system: Barbados data, *Quat. Res.*, *2*(3), 368–373.
Matthews, R. K. (1973), Relative elevation of late Pleistocene high sea level stands: Barbados uplift rates and their implications, *Quat. Res.*, *3*(1), 147–153.
McManus, J. F., R. Francois, J. M. Gherardi, L. D. Keigwin, and S. Brown-Leger (2004), Collapse and rapid resumption of Atlantic meridional circulation linked to deglacial climate changes, *Nature*, *428*(6985), 834–837.
McNeall, D., P. R. Halloran, P. Good, and R. A. Betts (2011), Analyzing abrupt and nonlinear climate changes and their impacts, *Wiley Interdiscip. Rev.: Clim. Change*, *2*(5), 663–686.
Mesolella, K. J. (1967), Zonation of uplifted Pleistocene coral reefs on Barbados, West Indies, *Science*, *156*(3775), 638–640.
Mesolella, K. J., R. K. Matthews, W. S. Broecker, and D. L. Thurber (1969), The astronomical theory of climatic change: Barbados data, *J. Geol.*, *77*(3), 250–274.
Milankovitch, M. (1941), *Canon of Insolation and the Ice-Age Problem*, *Spec. Pub. of the R. Serb. Acad.* [in German], vol. 132, 484 pp., Israel Program for Sci. Transl, Jerusalem.
Miller, G. H. (1980), Late Foxe glaciation of southern Baffin Island, N.W.T., Canada, *Geol. Soc. Am. Bull.*, *91*(7), 399–405.
Milne, G. A., and J. X. Mitrovica (2008), Searching for eustasy in deglacial sea-level histories, *Quat. Sci. Rev.*, *27*(25–26), 2292–2302.
Mitrovica, J. X., A. M. Forte, and M. Simons (2000), A reappraisal of postglacial decay times from Richmond Gulf and James Bay, Canada, *Geophys. J. Int.*, *142*(3), 783–800.
Monnin, E., A. Indermühle, A. Dällenbach, J. Flückiger, B. Stauffer, T. F. Stocker, D. Raynaud, and J.-M. Barnola (2001), Atmospheric CO_2 concentrations over the last glacial termination, *Science*, *291*(5501), 112–114.
Murton, J. B., M. D. Bateman, S. R. Dallimore, J. T. Teller, and Z. Yang (2010), Identification of Younger Dryas outburst flood path from Lake Agassiz to the Arctic Ocean, *Nature*, *464*, 740–743.
Nakada, M., and K. Lambeck (1988), The melting history of the late Pleistocene Antarctic ice sheet, *Nature*, *333*(6168), 36–40.
Okuno, J., and H. Miura (2013), Last deglacial relative sea level variations in Antarctica derived from glacial isostatic adjustment modelling, *Geosci. Front.*, *4*(6), 623–632.
Pearce, C., M.-S. Seidenkrantz, A. Kuijpers, and N. F. Reynisson (2014), A multi-proxy reconstruction of oceanographic conditions around the Younger Dryas—Holocene transition in Placentia Bay, Newfoundland, *Mar. Micropaleontol.*, *112*, 39–49.
Peltier, W. R. (1974), The impulse response of a Maxwell Earth, *Rev. Geophys.*, *12*, 649–669.
Peltier, W. R. (2004), Global glacial isostasy and the surface of the Ice-Age Earth: The ICE-5G (VM2) Model and GRACE, *Annu. Rev. Earth Planet. Sci.*, *32*(1), 111–149.
Peltier, W. R., and R. G. Fairbanks (2006), Global glacial ice volume and Last Glacial Maximum duration from an extended Barbados sea level record, *Quat. Sci. Rev.*, *25*(23–24), 3322–3337.
Peteet, D. (1995), Global Younger Dryas, *Quat. Int.*, *28*, 93–104.

Piotrowski, A. M., S. L. Goldstein, S. R. Hemming, and R. G. Fairbanks (2005), Temporal relationships of carbon cycling and ocean circulation at glacial boundaries, *Science*, *307*(5717), 1933–1938.
Pirazzoli, P. A., and L. F. Montaggioni (1988), Holocene sea-level changes in French Polynesia, *Palaeogeogr. Palaeoclimatol. Palaeoecol.*, *68*(2–4), 153–175.
Ponel, P., E. Gandouin, G. R. Coope, V. Andrieu-Ponel, F. Guiter, B. Van Vliet-Lanoë, E. Franquet, M. Brocandel, and J. Brulhet (2007), Insect evidence for environmental and climate changes from Younger Dryas to Sub-Boreal in a river floodplain at St-Momelin (St-Omer basin, northern France), Coleoptera and Trichoptera, *Palaeogeogr. Palaeoclimatol. Palaeoecol.*, *245*(3–4), 483–504.
Pringault, O., R. De Wit, and G. Camoin (2004), Functioning of modern marine microbialites built by benthic cyanobacteria, *Microbiology*, *8*, 41–56.
Rainio, H., M. Saarnisto, and I. Ekman (1995), Younger Dryas end moraines in Finland and NW Russia, *Quat. Int.*, *28*, 179–192.
Rasmussen, S. O., et al. (2006), A new Greenland ice core chronology for the last glacial termination, *J. Geophys. Res.*, *111*, D06102, doi:10.1029/2005JD006079.
Renssen, H., A. Mairesse, H. Goosse, P. Mathiot, O. Heiri, D. M. Roche, K. H. Nisancioglu, and P. J. Valdes (2015), Multiple causes of the Younger Dryas cold period, *Nat. Geosci.*, *8*, 946–949.
Rind, D., D. Peteet, W. Broecker, A. McIntyre, and W. Ruddiman (1986), The impact of cold North Atlantic sea surface temperatures on climate: Implications for the Younger Dryas cooling (11–10 k), *Clim. Dyn.*, *1*(1), 3–33.
Rooth, C. (1982), Hydrology and ocean circulation, *Prog. Oceanogr.*, *11*(2), 131–149.
Ruddiman, W. F. (2001), *Earth's Climate Past and Future*, 465 pp., W. H. Freeman, New York.
Ruddiman, W. F., and A. McIntyre (1981), The North Atlantic Ocean during the last deglaciation, *Palaeogeogr. Palaeoclimatol. Palaeoecol.*, *35*, 145–214.
Scambos, T., H. A. Fricker, C.-C. Liu, J. Bohlander, J. Fastook, A. Sargent, R. Massom, and A.-M. Wu (2009), Ice shelf disintegration by plate bending and hydro-fracture: Satellite observations and model results of the 2008 Wilkins ice shelf break-ups, *Earth Planet. Sci. Lett.*, *280*(1–4), 51–60.
Schellmann, G., and U. Radtke (2004), A revised morpho- and chronostratigraphy of the Late and Middle Pleistocene coral reef terraces on Southern Barbados (West Indies), *Earth Sci. Rev.*, *64*(3–4), 157–187.
Seager, R., D. S. Battisti, J. H. Yin, N. Gordon, N. Naik, A. Clement, and M. Cane (2002), Is the Gulf Stream responsible for Europe's mild winters?, *Q. J. R. Meteorol. Soc.*, *128*(586), 2563–2586.
Severinghaus, J. P., T. Sowers, E. J. Brook, R. B. Alley, and M. L. Bender (1998), Timing of abrupt climate change at the end of the Younger Dryas interval from thermally fractionated gases in polar ice, *Nature*, *391*(6663), 141–146.
Simpson, M., G. A. Milne, P. Huybrechts, and A. J. Long (2009), Calibrating a glaciological model of the Greenland ice sheet from the Last Glacial Maximum to present-day using field observations of relative sea level and ice extent, *Quat. Sci. Rev.*, *28*(17–18), 1631–1657.
Stanford, J. D., E. J. Rohling, S. E. Hunter, A. P. Roberts, S. O. Rasmussen, E. Bard, J. McManus, and R. G. Fairbanks (2006), Timing of meltwater pulse 1a and climate responses to meltwater injections, *Paleoceanography*, *21*, PA4103, doi:10.1029/2006PA001340.
Steffen, H., P. Wu, and H. Wang (2013), Optimal locations of sea-level indicators in glacial isostatic adjustment investigations, *Solid Earth Discuss.*, *5*(2), 2419–2448.
Stein, R., and K. Fahl (2012), Deglacial/Holocene variability of Arctic sea-ice cover and Younger Dryas event: Reconstruction from biomarker (IP25 and PIP25) data, Geophys. Res. Abstr., vol. *14*, EGU2012-1374-1, EGU General Assembly, Vienna, Austria, 22 - 27 April.
Sutherland, D., J. Gray, J. D. Peacock, M. Gordon, R. Walker, H. Tipping, H. Birks, A. Werritty, and L. McEwen (1993), *Quaternary of Scotland*, 695 pp., Springer, Netherlands.
Tarasov, L., and W. R. Peltier (2005), Arctic freshwater forcing of the Younger Dryas cold reversal, *Nature*, *435*, 662–665.
Taylor, F., and P. Mann (1991), Late Quaternary folding of coral reef terraces, Barbados, *Geology*, *19*(2), 103–106.
Taylor, K., G. W. Lamorey, G. A. Doyle, R. B. Alley, P. M. Grootes, P. A. Mayewski, J. W. C. White, and L. K. Barlow (1993), The 'flickering switch' of late Pleistocene climate change, *Nature*, *361*(6411), 432–436.
Taylor, K., et al. (1997), The Holocene-Younger Dryas transition recorded at Summit, Greenland, *Science*, *278*(5339), 825–827.
Teller, J. T. (1995), History and drainage of large ice-dammed lakes along the Laurentide Ice Sheet, *Quat. Int.*, *28*, 83–92.
Teller, J. T., M. Boyd, Z. Yang, P. S. G. Kor, and A. Mokhtari Fard (2005), Alternative routing of Lake Agassiz overflow during the Younger Dryas: New dates, paleotopography, and a re-evaluation, *Quat. Sci. Rev.*, *24*(16–17), 1890–1905.
Thomas, A. L., et al. (2012), Assessing subsidence rates and paleo water-depths for Tahiti reefs using U–Th chronology of altered corals, *Mar. Geol.*, *295–298*, 86–94.
Thompson, W. G., M. W. Spiegelman, S. L. Goldstein, and R. C. Speed (2003), An open-system model for U-series age determinations of fossil corals, *Earth Planet. Sci. Lett.*, *210*(1–2), 365–381.
Ullman, D. J., A. N. LeGrande, A. E. Carlson, F. S. Anslow, and J. M. Licciardi (2014), Assessing the impact of Laurentide Ice Sheet topography on glacial climate, *Clim. Past*, *10*(2), 487–507.
Walcott, R. I. (1972), Past sea levels, eustasy and deformation of the Earth, *Quat. Res.*, *2*(1), 1–14.
Watts, W. (1980), Regional variation in the response of vegetation to late glacial climatic events in Europe, in *Studies in the Late Glacial of Northwest Europe*, edited by J. Lowe, J. Gray, and J. Robinson, pp. 1–22, Pergamon, New York.
Weaver, A. J., O. A. Saenko, P. U. Clark, and J. X. Mitrovica (2003), Meltwater pulse 1A from Antarctica as a trigger of the Bolling-Allerod warm interval, *Science*, *299*(5613), 1709–1713.
Weyl, P. (1968), The role of the oceans in climate change: A theory of the ice ages, *Meteorol. Monogr.*, *8*, 37–62.
Winguth, C., D. M. Mickelson, E. Larsen, J. R. Darter, C. A. Moeller, and K. Stalsberg (2005), Thickness evolution of the Scandinavian Ice Sheet during the Late Weichselian in Nordfjord, western Norway: Evidence from ice-flow modeling, *Boreas*, *34*(2), 176–185.
Wunsch, C. (1998), The work done by the wind on the oceanic general circulation, *J. Phys. Oceanogr.*, *28*(11), 2332–2340.
Wunsch, C. (2002), What is the thermohaline circulation?, *Science*, *298*(5596), 1179–1181.
Yashayaev, I., and A. Clarke (2008), Evolution of North Atlantic water masses inferred from Labrador Sea salinity series, *Oceanography*, *21*(1), 30–45.
Yokoyama, Y., K. Lambeck, P. De Deckker, P. Johnston, and L. K. Fifield (2000), Timing of the Last Glacial Maximum from observed sea-level minima, *Nature*, *406*(6797), 713–716.
Yokoyama, Y., P. De Deckker, K. Lambeck, P. Johnston, and L. K. Fifield (2001), Sea-level at the Last Glacial Maximum: Evidence from northwestern Australia to constrain ice volumes for oxygen isotope stage 2, *Palaeogeogr. Palaeoclimatol. Palaeoecol.*, *165*(3–4), 281–297.